Interface-enhanced continuous 2D-carbon network enabling high-performance Si anodes for Li-ion batteries

Jiaying Peng,[a,b] Rong Shao,[a,b] Sijie Huang,[a] Zhenjiang Cao,[a] Tianren Zhang,[c] Yinliang Cao,[c] Shuguo Zhang,[c] Chunchuan Xu,[c] Yongzheng Shi,[a,b] Jin Niu,[a,b,*] Feng Wang[a,b,*]

[a] State Key Laboratory of Chemical Resource Engineering, Laboratory of Electrochemical Process and Technology for materials, Beijing University of Chemical Technology, Beijing, 100029, P. R. China

[b] Beijing Advanced Innovation Center for Soft Matter Science and Engineering, Beijing University of Chemical Technology, Beijing, 100029, P. R. China

[c] Tianneng Battery Group Co., Ltd. Zhejiang, 313100, P. R. China

*Corresponding authors.

E-mail: niujin@mail.buct.edu.cn; wangf@mail.buct.edu.cn

Material characterization. SEM (JEOL, JSM-6701F) and TEM (JEOL, JSM-2100) were used to characterize the morphologies of the electrodes. The elemental distributions were characterized by STEM (JEOL, JEM-ARM200F) and EDX spectroscopy. The electrodes after cycling were sonicated in the dimethyl carbonate (DMC) to remove the active material from the collector and mounted on a grid, which was then sealed in Ar-filled transfer vessels for immediate TEM observation. The crystal phases of the samples were analyzed by XRD (Rigaku RINT 200V/PC) using Cu Ka radiation. Raman spectra were obtained using a LabRam HR800 spectrometer. XPS data were obtained using an ESCALAB 250 system with monochromatic Al K X-ray sources.

Electrochemical measurements. For the preparation of anodes, the active materials (Si@GCNS, Si-GCNS, or Si@GC) were weighed with sodium alginate and acetylene black in a ratio of 8:1:1 and evenly mixed into slurry, which was then coated on Cu foils and dried at 60 °C for 24 h under vacuum. The loading mass of the active material for the anode is 1.5-2 mg cm^{-2}. For the preparation of the cathode, the active materials (LFP) was weighed with PVDF and acetylene black in a ratio of 8:1:1 and evenly mixed into slurry, which was coated on Al foil and dried at 80 °C for 24 h under vacuum. For the half-cell tests, the electrochemical properties were evaluated using a CR2032 coin-type cell. A Li metal foil was used as the counter and reference electrode. A Celgard 2400 polypropylene membrane was used as the separator. The electrolyte was 1 M LiPF$_6$ in a mixture of ethylene carbonate (EC), dimethyl carbonate (DMC), diethyl carbonate (DEC) (1:1:1 by vol) with 5 wt% fluoroethylene carbonate (FEC). All the

electrochemical tests were carried out at room temperature. For the anode tests, GCD measurements were performed on a Land Battery Tester (Land CT2001A system) at various current densities from 0.2 to 5 A g^{-1} in the potential range from 0.01 to 1.5 V. GITT tests were carried out using a constant current pulse with a duration of 10 min and a relaxation process over 10 min. CV measurements were performed with sweep rates from 0.2 to 1.2 mV s^{-1} using a CHI660E work station. The frequency for the EIS measurements ranged from 100 kHz to 10 mHz. For *in-situ* Raman spectroscopy measurements, Si@GCNS was coated on a copper foam using sodium alginate as a binder (with a weight ratio of 9:1).

The LFP cathode and the Si@GCNS anode were used to assemble a full pouch cell with an N/P ratio of 1.1 using the same electrolyte and separator for half cell. The loading mass of the LFP cathode is ~15 mg cm^{-2}. The loading mass of the Si anode is ~1 mg cm^{-2}. GCD tests were conducted at 1 A g^{-1} (based on the weight of anode material) within the voltage range of 2.5-4.2 V. The specific capacity of the full cell was calculated based on the weight of the cathode material. The energy density of the full cell was calculated based on the total weight of the cathode and anode materials.

COMSOL Multiphysics simulation. Current density distributions were simulated based on COMSOL Multiphysics 5.6. The two-dimensional transient model and tertiary Nernst-Planck were chosen to simulate the Li-ion concentration distribution. The model of Si@GCNS is made up of a tightly packed layer of 4x4 spheres with one layer. The model of Si@GC is made up of 4x4 spheres with four tightly packed layers. The model of Si@GC is made up of layer disordered spheres with

one layer. Si surface is set to have low conductivity and the carbon surface is set to have

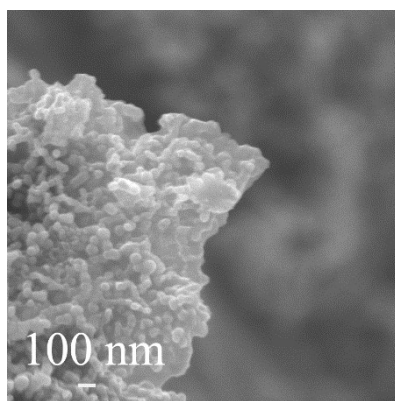high conductivity. The number of participating electrons is set to 1.
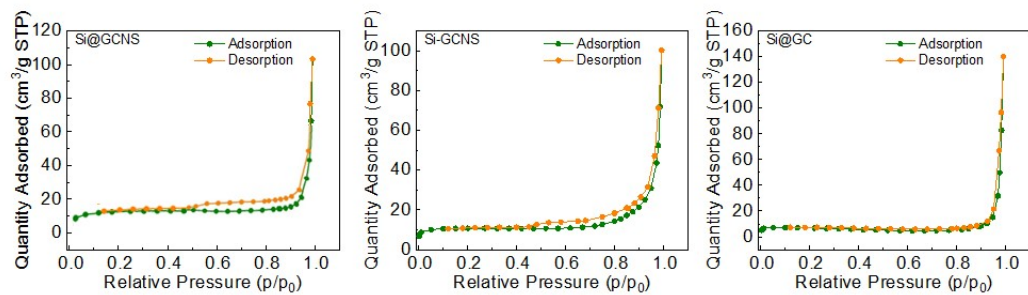
Figure S1 SEM image of Si@GCNS.

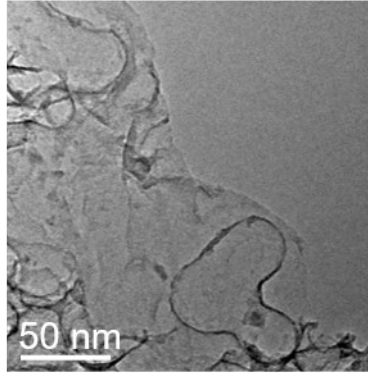Figure S2 N$_2$ adsorption/desorption isotherm plots of Si@GCNS, Si-GCNS, and Si@GC.

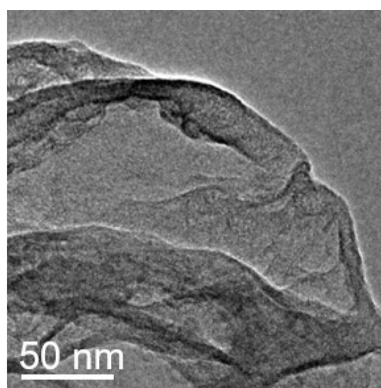Figure S3 TEM image of Si@GCNS after removing the Si from the nanosheet by alkali.

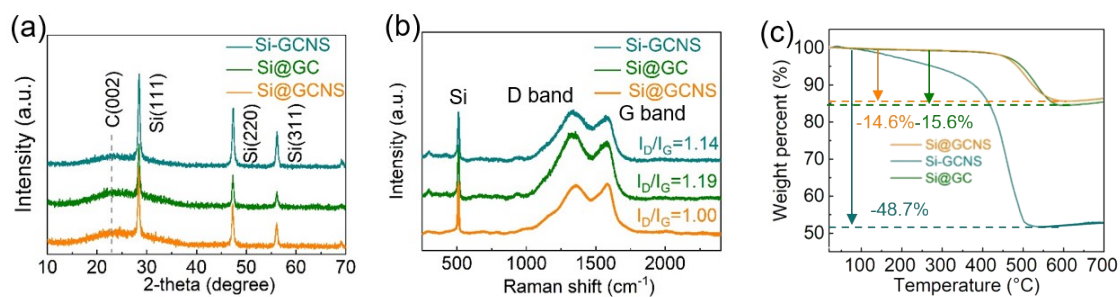Figure S4 TEM image of Si-GCNS after removing the Si from the nanosheet by alkali.

Figure S5 (a) XRD patterns, (b) Raman spectra, and (c) TG curves in an air atmosphere of Si@GCNS, Si-GCNS and Si@GC.

It should be noted that less weight of Si was used to prepare Si-GCNS to realize good loading effect. The ratio of Si to GCNS was determined based on the previously reported work [S1]. Based on the composition of Si@GCNS and KCl dosage, the yields of the composite are ~84% and ~49 % including and excluding KCl, respectively.
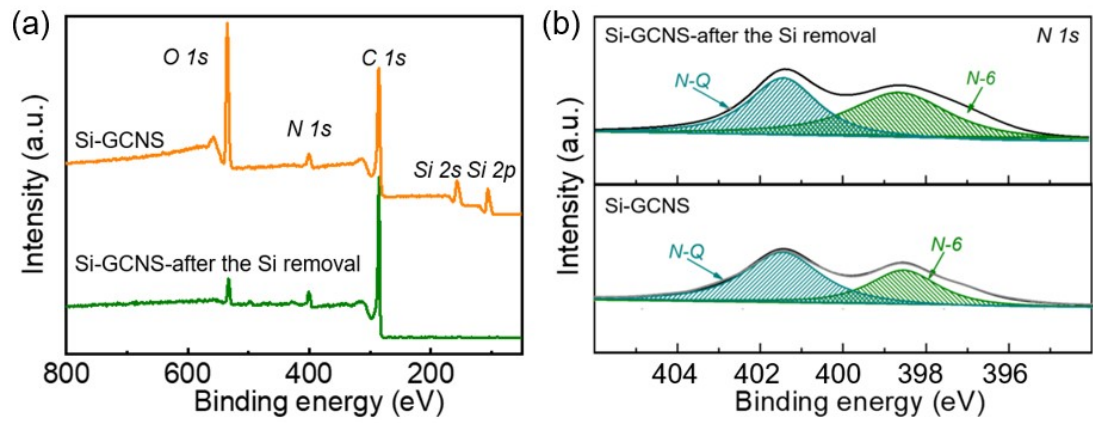
Figure S6 (a) XPS spectra and high-resolution (b) N 1s XPS spectra of Si-GCNS before and after removing Si.
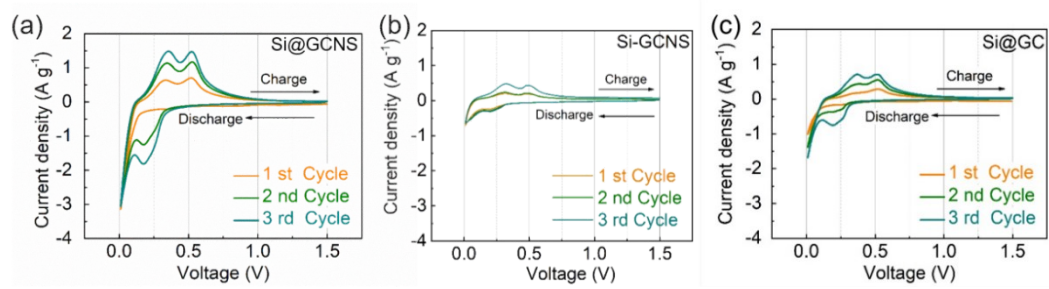
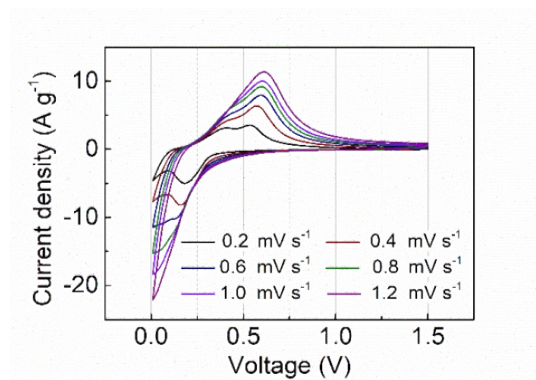Figure S7 CV curves at 0.2 mV s^{-1} of the (a) Si@GCNS, (b) Si-GCNS, and (c) Si@GC anodes.

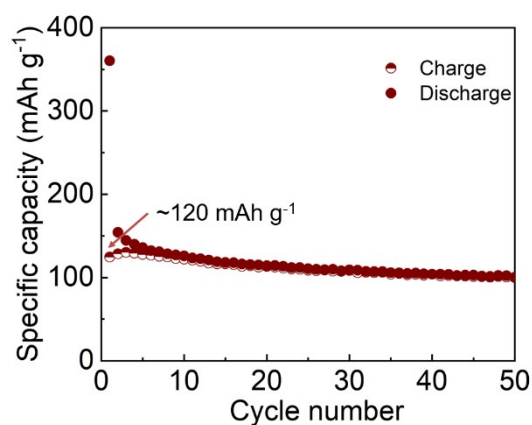Figure S8 CV curves of the Si@GCNS anode at different scan rates (0.2-1.2 mV s^{-1}).

Figure S9 Cycling performance of the GCNS (or GC) anode at the current density of 0.2 A g^{-1}.

The capacity of pure Si for all the anode at 0.2 A g^{-1} were calculated based on the content and capacity of GCNS (or GC). The Si within the Si@GCNS anode still showed the highest capacity of 3463 mAh g^{-1} among all the anodes (2134 mAh g^{-1} for Si within the Si@GC anode and 1615 mAh g^{-1} for Si within the Si-GCNS anode). The anode performance of the Si@GC anode was also better than that of the Si-GCNS anode.
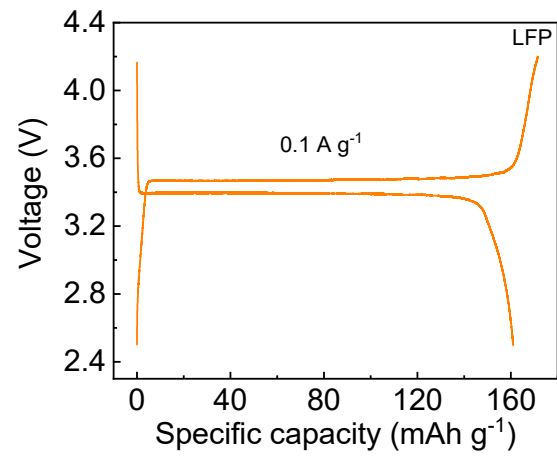
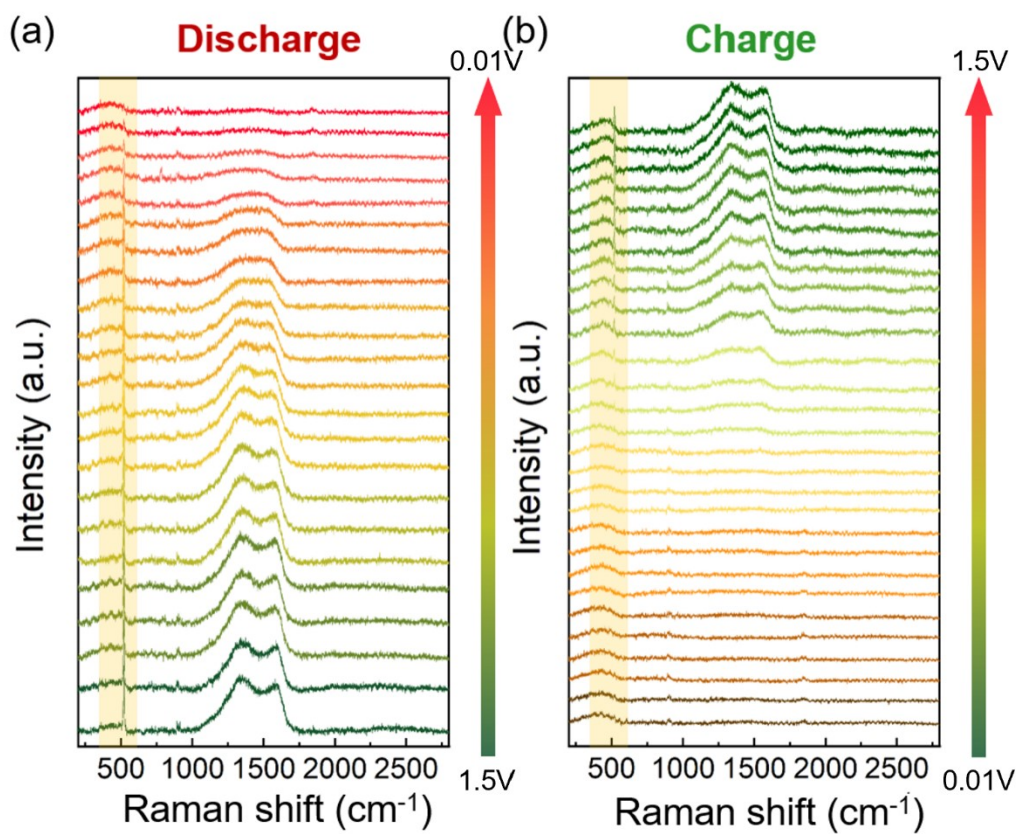Figure S10 GCD profiles of the LFP cathode in half cell using Li metal anode.

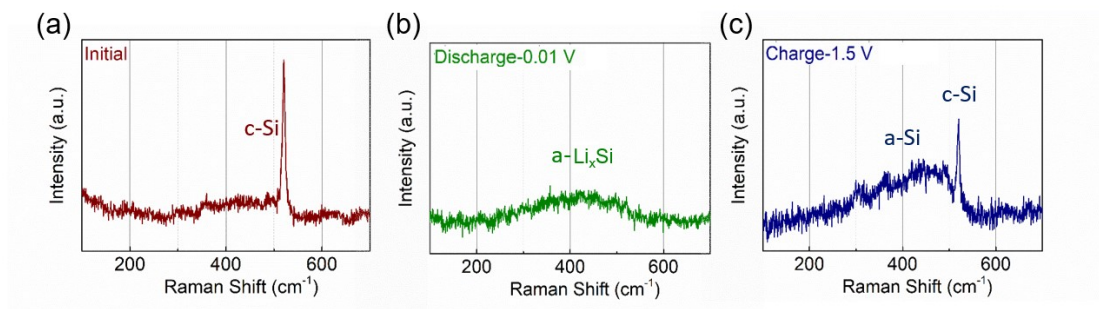Figure S11 In-situ Raman spectra of the Si@GCNS anode.

Figure S12 In-situ Raman spectra of the Si@GCNS anode at different charge-discharge states.
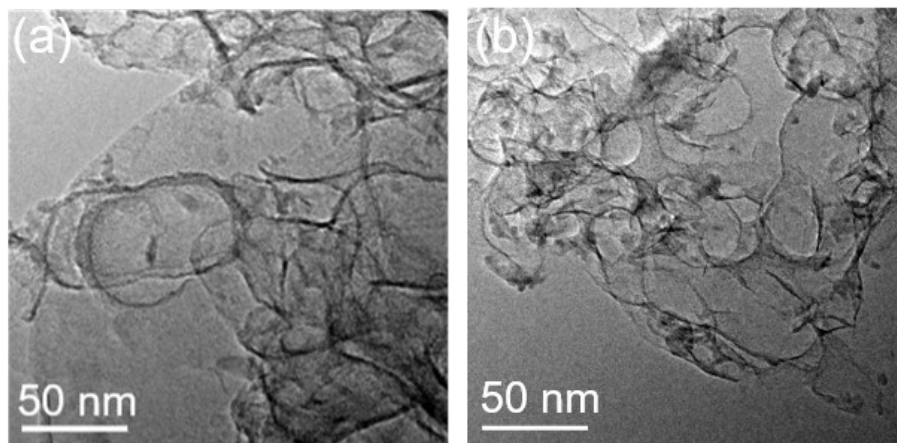
Figure S13 TEM images of the Si@GCNS anode after (a) 5 cycles and (b) 400 cycles
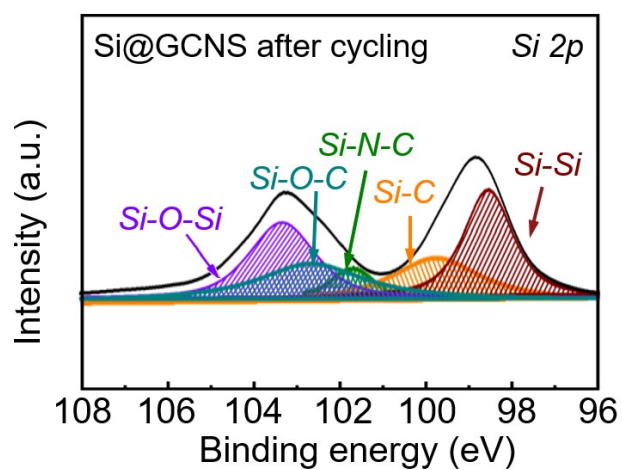
(Si was removed by alkali).

Figure S14 High-resolution Si 2p XPS spectrum of the Si@GCNS anode after 400 cycles (XPS was performed after sputtering with a depth of 20 nm to remove the SEI).
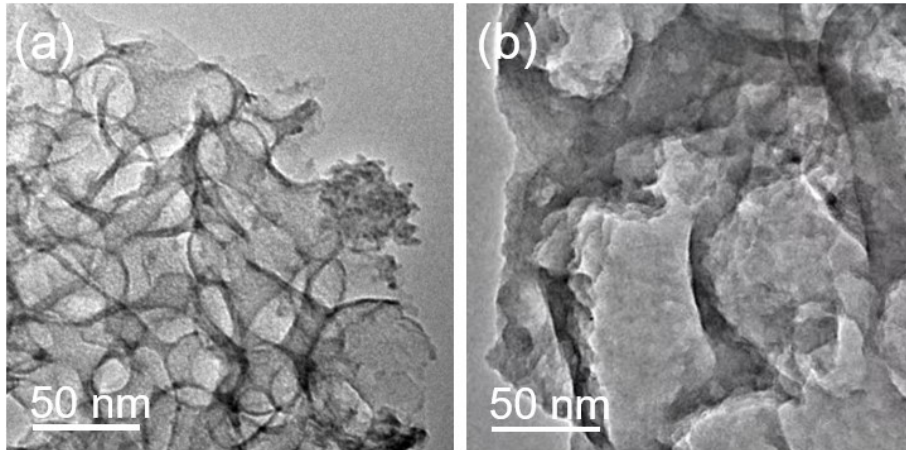
Figure S15 TEM images of the Si@GC anode (a) before and (b) after cycling (Si was removed by alkali).
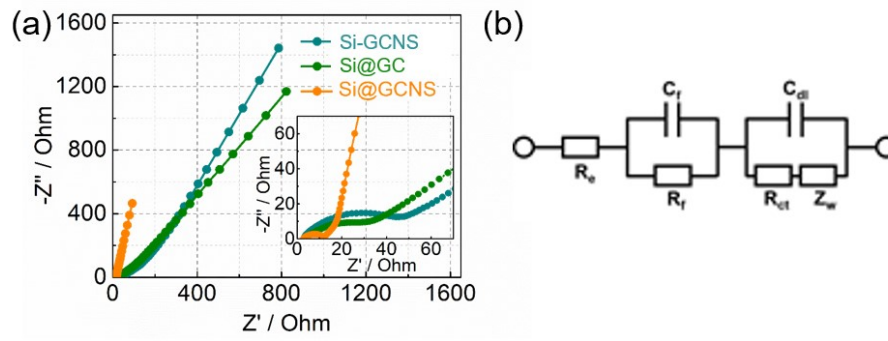
Figure S16 (a) Nyquist plots of the Si@GCNS, Si-GCNS, and Si@GC anode. (b) Equivalent-circuit diagram.
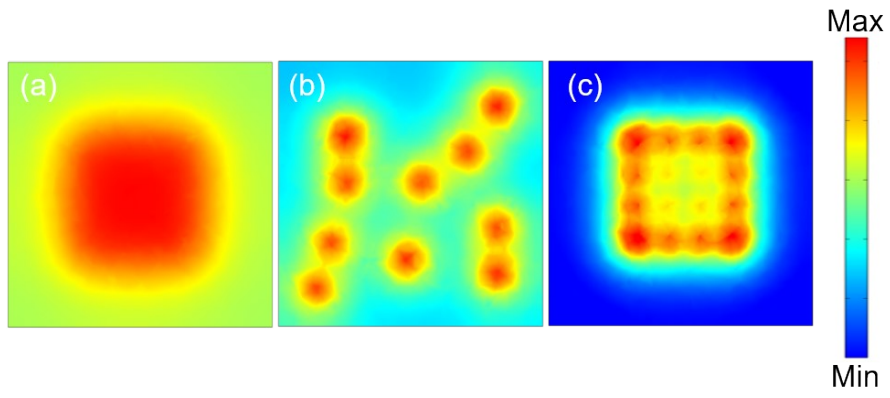
Figure S17 Top view of COMSOL simulation of Li-ion concentration distribution of (a) Si@GCNS, (b) Si-GCNS, and (c) Si@GC.

Table S1. Comparison of the electrochemical performance for Si-based anodes.

Sample	ICE (%)	Specific capacity (mAh g^{-1})	Specific capacity at high current density (mAh g^{-1})	Cycle number	Retention (%)	References[a]
Si@GCNS	**83.0**	**2975 @ 0.2 A g^{-1}**	**1892 @ 5.0 A g^{-1}**	**400@ 2.0 A g^{-1}**	**83.4**	**This Work**
Si/LM@C-CNF	87.4	2310 @ 0.1 A g^{-1}	613 @ 5.0 A g^{-1}	150@ 5.0 A g^{-1}	40.5	34
Ni-SiO$_2$/C HS	76.0	1185 @ 0.2 A g^{-1}	213 @ 2.0 A g^{-1}	200@ 0.2 A g^{-1}	44.9	35
SiO$_x$/C HS-TA	70.8	1200 @ 0.1 A g^{-1}	236.4 @ 3.0 A g^{-1}	100@ 0.1 A g^{-1}	58.3	36
SiO$_x$@Si/rGO	70.6	1992.4 @ 0.3 A g^{-1}	1180.2 @ 4.0 A g^{-1}	100@ 0.2 A g^{-1}	46.4	37
3D-Si@SiO$_x$/C	80.0	1635 @ 0.2 A g^{-1}	1500 @ 4.0 A g^{-1}	100@ 0.4 A g^{-1}	83.3	38
SGC	-	2025.6 @ 0.5 A g^{-1}	600 @ 5.0 A g^{-1}	380@ 0.5 A g^{-1}	83.3	39

[a]The reference numbers are corresponding to those in the manuscript.

Table S2. Comparison of the electrochemical performances for LIBs.

Electrodes	Energy density (Wh kg^{-1})	Cycle number	Retention (%)	References[a]
Si@GCNS//LFP	**460**	**300@1.0 A g^{-1}**	**89.8**	**This Work**
NCM//SiO$_x$@CNTs/C-550	325	200@ 0.1 C	70.0	40
LFP//Si p-NS@TNSs	405	80@ 0.1 A g^{-1}	78.8	41
SiO$_x$@Si/rGO	375.2	100@ 1.0 A g^{-1}	64.3	37
p-Si@C//LFP	381.61	200@ 0.2 C	68.7	42
PCC-nSi-2//NCM622	335.3	200@ 1.0 C	66.7	43
SLLIB–MCMB//LFP	302	300@ 0.2 C	46.6	44

[a]The reference numbers are corresponding to those in the manuscript.

Table S3. The simulation results of EIS for the Si/C anodes.

Sample	ESR (R_1, Ω)	R_f (R_2, Ω)	R_{ct} (R_3, Ω)
Si@GC	3.8	4.9	17.4
Si-GCNS	4.6	6.7	18.8
Si@GCNS	3.1	2.3	4.7

References

[S1] M. Yang, J. Liu, S. Li, S. Zhang, Y. Wang and C. He, Nano Energy, 2019, **65**, 104028.